Lindsey E. Padgett,[1] Brian Anderson,[1] Chao Liu,[2] Douglas Ganini,[3] Ronald P. Mason,[3] Jon D. Piganelli,[4] Clayton E. Mathews,[2] and Hubert M. Tse[1]

Loss of NOX-Derived Superoxide Exacerbates Diabetogenic CD4 T-Cell Effector Responses in Type 1 Diabetes

Diabetes 2015;64:4171–4183 | DOI: 10.2337/db15-0546

Reactive oxygen species (ROS) play prominent roles in numerous biological systems. While classically expressed by neutrophils and macrophages, CD4 T cells also express NADPH oxidase (NOX), the superoxide-generating multisubunit enzyme. Our laboratory recently demonstrated that superoxide-deficient nonobese diabetic (NOD.*Ncf1*^{m1J}) mice exhibited a delay in type 1 diabetes (T1D) partially due to blunted IFN-γ synthesis by CD4 T cells. For further investigation of the roles of superoxide on CD4 T-cell diabetogenicity, the NOD.BDC-2.5.*Ncf1*^{m1J} (BDC-2.5.*Ncf1*^{m1J}) mouse strain was generated, possessing autoreactive CD4 T cells deficient in NOX-derived superoxide. Unlike NOD.*Ncf1*^{m1J}, stimulated BDC-2.5.*Ncf1*^{m1J} CD4 T cells and splenocytes displayed elevated synthesis of Th1 cytokines and chemokines. Superoxide-deficient BDC-2.5 mice developed spontaneous T1D, and CD4 T cells were more diabetogenic upon adoptive transfer into NOD.*Rag* recipients due to a skewing toward impaired Treg suppression. Exogenous superoxide blunted exacerbated Th1 cytokines and proinflammatory chemokines to approximately wild-type levels, concomitant with reduced IL-12Rβ2 signaling and P-STAT4 (Y693) activation. These results highlight the importance of NOX-derived superoxide in curbing autoreactivity due, in part, to control of Treg function and as a redox-dependent checkpoint of effector T-cell responses. Ultimately, our studies reveal the complexities of free radicals in CD4 T-cell responses.

Type 1 diabetes (T1D) is characterized by a loss of self-tolerance, in which T-cells destroy insulin-secreting pancreatic β-cells. Currently, no cure exists for this disease; meanwhile, the worldwide incidence is steadily climbing by 4.7% per year in developed countries (1,2). CD4 T cells have classically been considered to be of chief importance in T1D, as CD4 T cell–deficient nonobese diabetic (NOD) mice are protected from T1D onset (3,4).

Superoxide synthesis is mediated by NADPH oxidase (NOX), a heme-containing multisubunit enzyme composed of cytosolic (p67^{phox}, p47^{phox}, p40^{phox}, and Rac1/2) and membrane-associated components (p22^{phox} and gp91^{phox}) (5). Normally localized in the cytosol in a quiescent state, the p47^{phox} subunit of NOX migrates to the membrane upon activation and associates with other components of the NOX machinery, inducing production of superoxide, which is quickly dismutated to form hydrogen peroxide (6). Reactive oxygen species (ROS) are classically known to possess potent antimicrobial properties, but ROS are also powerful modulators of the immune response (7).

Studies by our laboratory and others have demonstrated ROS function as a proinflammatory-derived third signal to synergize innate with adaptive immune responses (8–13). ROS promote proinflammatory cytokine and type I interferon synthesis via the redox-sensitive mitogen-activated protein kinase, nuclear factor-κB, and activator protein-1 signaling pathways (8,9,14,15). We previously reported that NOD mice possessing a spontaneous point mutation (*Ncf1*^{m1J}), resulting in a premature truncation of the p47^{phox} NOX subunit (16), were protected against T1D onset due, in part, to attenuated

[1]Department of Microbiology, Comprehensive Diabetes Center, University of Alabama at Birmingham School of Medicine, Birmingham, AL
[2]Department of Pathology, Immunology, and Laboratory Medicine, University of Florida College of Medicine, Gainesville, FL
[3]Free Radical Metabolites, Immunity, Inflammation and Disease Laboratory, National Institutes of Environmental Health Sciences, National Institutes of Health, Research Triangle Park, NC
[4]Department of Surgery, Immunology, and Pathology, University of Pittsburgh School of Medicine, Pittsburgh, PA

Corresponding author: Hubert M. Tse, htse@uab.edu.

Received 23 April 2015 and accepted 4 August 2015.

This article contains Supplementary Data online at http://diabetes.diabetesjournals.org/lookup/suppl/doi:10.2337/db15-0546/-/DC1.

antiviral innate immune responses (17), dysregulated CD4 and CD8 T-cell responses (10,18,19), and an enhancement in alternatively activated M2 macrophages (19).

We sought to further examine the role of NOX-derived ROS in diabetogenic CD4 T-cell effector responses using the NOD.BDC-2.5 (BDC-2.5) mouse strain. The BDC-2.5 mouse is an invaluable tool for dissecting the role of a single CD4 T-cell clone in T1D (20,21). Recognizing chromogranin A (22), a protein component of the islet secretory granules, BDC-2.5 CD4 T cells are intrinsically activated to a Th1-like phenotype and destroy pancreatic β-cells by recruiting classically activated M1 macrophages (23,24). Here, we report that stimulated BDC-2.5.*Ncf1*^{m1J} splenocytes and CD4 T cells exhibited exacerbated proinflammatory cytokine and chemokine production, with a concomitant increase in spontaneous T1D and enhanced diabetogenicity upon transfer into NOD.*Rag* recipients. This heightened diabetogenicity was due in part to less suppressive T-regulatory (Treg) cells. Addition of an exogenous superoxide generator blunted Th1 autoreactive immune effector responses within BDC-2.5.*Ncf1*^{m1J} CD4 T cells by curbing interleukin-12 receptor β2 (IL-12Rβ2) signaling and attenuating P-signal transducer and activator of transcription 4 (STAT4) (Y693) activation. These results demonstrate the dual roles of superoxide in functioning as a proinflammatory third signal for efficient adaptive immune maturation but also in restricting autoreactive CD4 T-cell responses.

RESEARCH DESIGN AND METHODS

Animals

NOD.Cg-Ncf1m1J/Mx (NOD.*Ncf1*^{m1J}), NOD.Cg-Tg (TcraBDC2.5,TcrbBDC2.5)/DoiJ (BDC-2.5), and NOD.129S7 (B6)-*Rag1*^{tm1Mom}/J (NOD.*Rag*) mice were bred and housed under pathogen-free conditions in the Research Support Building animal facility at the University of Alabama at Birmingham. BDC-2.5 mice were originally obtained from Kathryn Haskins at the National Jewish Hospital (Denver, CO), and NOD.*Rag* mice were purchased from The Jackson Laboratory (Bar Harbor, ME). Mice were maintained on a light/dark (12/12 h) cycle at 23°C and received continuous access to standard laboratory chow and acidified water. Age- and sex-matched BDC-2.5 and BDC-2.5.*Ncf1*^{m1J} mice were used for all experiments and in accordance with the University of Alabama at Birmingham and University of Florida Institutional Animal Care and Use Committee.

Materials

Anti–γ-interferon (IFN-γ), –interleukin (IL)-2, –IL-10, and –IL-17A antibody pairs for ELISA; fluorochrome-conjugated anti-CD4, -CD8, -B220, -Vβ4, -Vβ5, -Vβ8, -CD11b, and -CD11c antibodies for fluorescence-activated cell sorter (FACS); and anti-CD3ε and anti-CD28 antibodies were purchased from BD Biosciences. IL-1β, CCL5, and tumor necrosis factor (TNF)-α DuoSet ELISA kits, CXCL10 antibody pairs, and fluorochrome-conjugated anti–IL-12Rβ2 were purchased from R&D Systems. Fluorochrome-conjugated anti-CD19, -CD25, -CD44, and -CD69 antibodies were purchased from eBioscience, while biotin anti-mouse CD4, in addition to anti-F4/80 fluorochrome-conjugated and live/dead fluorochrome-conjugated antibodies, was purchased from Invitrogen. Anti–P-STAT4 (Y693) antibody was purchased from Cell Signaling, while anti-STAT4 antibody was obtained from Biolegend. The BDC-2.5 mimotope (EKAHRPIWARMDAKK) was synthesized by the University of Alabama at Birmingham peptide synthesis core facility. Xanthine oxidase and β-actin were obtained from Sigma-Aldrich, and r-hIL-2 was purchased from Peprotech.

Generation of the BDC-2.5.*Ncf1*^{m1J} Mouse

NOD.BDC-2.5.*Ncf1*^{m1J} (BDC-2.5.*Ncf1*^{m1J}) mice were generated by crossing BDC-2.5 (21) to NOD.*Ncf1*^{m1J} (10) mice followed by intercrossing of the F1 progeny. F2 progeny homozygous for the *Ncf1*^{m1J} mutation (10) and the BDC-2.5 transgene (21) were used to establish this strain. The inability to synthesize superoxide did not affect lymphocyte development and differentiation in BDC-2.5.*Ncf1*^{m1J} mice, as lymphocyte population percentages revealed equivalent expression of Vβ4, CD4 T cells (Supplementary Fig. 2*A*) within superoxide-sufficient and -deficient strains according to the gating strategy depicted in Supplementary Fig. 1. No differences were observed in the percentages of B cells (Supplementary Fig. 2*B*), macrophages (Supplementary Fig. 2*C*), dendritic cells (Supplementary Fig. 2*D*), and regulatory CD4 T cells (Supplementary Fig. 2*E*).

Luminol Oxidation to Detect Superoxide Synthesis

The redox-sensitive substrate luminol was used to detect superoxide synthesis (17). BDC-2.5 and BDC-2.5.*Ncf1*^{m1J} splenocytes and CD4 T cells were seeded onto 96-well polystyrene round-bottom plates with 200 μmol/L luminol (Sigma-Aldrich), 0.32 units/mL horseradish peroxidase (Sigma-Aldrich), 100 ng/mL phorbol 12-myristate 13-acetate (PMA), and 1 μg/mL ionomycin or 1 μmol/L BDC-2.5 Mimotope (9). Luminescence was quantified using a SpectraMax L Luminescence microplate reader with readings every 2 min for 60 min.

Immuno-Spin Trapping and Immunofluorescence

Macromolecular-centered free radicals were detected upon stimulating splenocytes with 1 μmol/L BDC-2.5 mimotope in the presence of 1 mmol/L 5,5-dimethyl-1-pyrroline *N*-oxide (DMPO; Dojindo) in tissue culture–treated chamber slides. Cells were fixed in 4% paraformaldehyde in PBS, permeabilized with 0.5% Triton X-100 in PBS, blocked with 5% BSA in PBS, and incubated with 20 μg/mL of chicken IgY anti-DMPO as previously described (25,26). DMPO adducts were detected with Alexa Fluor 488–conjugated goat anti-chicken IgY secondary antibody (1:500; Invitrogen). P-STAT4 (Y693) and STAT4 were detected with Alexa Fluor 488–conjugated donkey anti-rabbit IgG (H+L) secondary antibody (1:500) and Cy3-conjugated Donkey anti-mouse IgG (H+L) (1:500) (Jackson Immunoresearch), respectively. CD4 T cells were identified with Alexa Fluor 647–conjugated

streptavidin secondary antibody (1:500; Life Technologies). Images were obtained with an Olympus IX81 Inverted Microscope at a 40× objective and analyzed with cellSens Dimension imaging software, version 1.12. For quantitation of fluorescence intensity, three to six images were obtained for each data point. Each image was collected at the same exposure time, adjusted to the same intensity level for standardization, and the fluorescence intensity was measured using ImageJ software (National Institutes of Health).

Analysis of Lymphocyte Populations, Activation Markers, and IL-12Rβ2 by Flow Cytometry

According to the gating strategies shown in Supplementary Figs. 1 and 5, BDC-2.5 and BDC-2.5.*Ncf1*^{m1J} splenic single cell suspensions were surface stained in FACS buffer (1% BSA in PBS) with appropriately diluted fluorochrome-conjugated antibodies and isotype controls (BD Biosciences, eBioscience, and R&D) (Supplementary Figs. 6 and 10) (17). One hundred thousand cell events were collected with the FACSCalibur, and data were analyzed with FlowJo, version 9.6.1, software (Tree Star Incorporated).

CD4 T-Cell Purification, Polyclonal Stimulation, Primary Recall Assays, Greiss Assay, ELISAs, and 3-(4,5-dimethylthiazol-2-yl)-2,5-diphenyltetrazolium bromide Assay

Splenic CD4 T cells from BDC-2.5 and BDC-2.5.*Ncf1*^{m1J} mice were purified by negative selection according to the manufacturer's protocol using the EasySep CD4 T-cell enrichment kit (STEMCELL Technologies). CD4 T-cell purity was routinely assessed by flow cytometry and found to be >90% (data not shown). T cells were stimulated with plate-bound anti-CD3ε (0.1 μg/mL) and anti-CD28 (1 μg/mL), and exogenous superoxide was added via 1 mU/mL xanthine oxidase (XO) (17). BDC-2.5 and BDC-2.5.*Ncf1*^{m1J} splenocytes were incubated with 1 μmol/L BDC-2.5 mimotope or 10^4 dispersed NOD.*Rag* islet cells in the presence or absence of 1 mU/mL XO (9,15). Greiss assay and ELISAs were read on a Synergy2 microplate reader with Gen5, version 1.10, software (BioTek) as previously described (17). 3-(4,5-dimethylthiazol-2-yl)-2,5-diphenyltetrazolium bromide (MTT) assay to assess T-cell proliferation was performed according to the manufacturer's protocol (Sigma-Aldrich).

Adoptive Transfer of Type 1 Diabetes and In Vivo Suppression Assay

Adoptive transfer of purified CD4 T cells into NOD.*Rag* recipients was performed as described previously (10,27). BDC-2.5 and BDC-2.5.*Ncf1*^{m1J} Tregs were purified via negative selection, stained with fluorescein isothiocyanate–labeled anti–glucocorticoid-induced tumor necrosis factor receptor–related protein and phycoerythrin-labeled anti-CD25. The CD25/GITR double-positive Treg population was sorted with a BD FACSAria III (BD Biosciences). The percentage of Foxp3$^+$ Treg cells isolated after sorting was similar between BDC-2.5 and BDC-2.5.*Ncf1*^{m1J} (Supplementary Fig. 8). Polyclonally stimulated BDC-2.5 CD4 T cells were used as effector cells. Stimulated-BDC-2.5 CD4 effector T cells (10^5) were transferred intraperitoneally, either alone or cotransferred with BDC-2.5 or BDC-2.5.*Ncf1*^{m1J} Tregs (2×10^4), into NOD.*Rag* mice and monitored for T1D as described.

Statistical Analysis

Data were analyzed via GraphPad Prism, version 5.0, statistical software. The difference between mean values for each experimental group was assessed using the two-tailed Student *t* test with $P < 0.05$ considered significant.

RESULTS

BDC-2.5.*Ncf1*^{m1J} CD4 T Cells and Splenocytes Exhibited a Dampened Respiratory Burst

For exploration of the role of NOX-derived superoxide on diabetogenic CD4 T-cell effector responses, the BDC-2.5.*Ncf1*^{m1J} mouse strain was generated, and luminol oxidation by BDC-2.5 and BDC-2.5.*Ncf1*^{m1J} splenocytes was used to corroborate the deficiency in NOX-derived superoxide (Fig. 1*A*). Stimulated BDC-2.5.*Ncf1*^{m1J} splenocytes displayed a 21-fold reduction in chemiluminescence compared with BDC-2.5 splenocytes with luminol and horseradish peroxidase (HRP). To validate blunted free radical synthesis within the CD4 T-cell compartment, we stimulated BDC-2.5 and BDC-2.5.*Ncf1*^{m1J} CD4 T cells with PMA/ionomycin in the presence of luminol and HRP (Fig. 1*B*). Primary human and mouse CD4 T cells have been shown to express a functional phagocyte type NOX, and T-cell receptor (TCR) stimulation elicits rapid production of superoxide and hydrogen peroxide (28). Similar to splenocytes, luminol oxidation by stimulated BDC-2.5.*Ncf1*^{m1J} CD4 T cells was decreased 1.4-fold compared with BDC-2.5 CD4 T cells, confirming the blunted respiratory burst capacity from our previous studies using CD4 or CD8 T lymphocytes (10,18).

BDC-2.5.*Ncf1*^{m1J} CD4 T Cells Displayed Blunted Cellular Self-Oxidation

For further demonstration that NOX enzymatic activity was curtailed in the absence of NOX-derived superoxide, immuno-spin trapping using the free radical spin trap DMPO was performed to quantify the self-oxidation of BDC-2.5 and BDC-2.5.*Ncf1*^{m1J} splenocytes (Fig. 2). The formation of free radicals in macromolecules of the cells results in the formation of stable DMPO adducts that were imaged and quantified. The BDC-2.5 mimotope elicited an increase in DMPO-adduct formation by BDC-2.5 CD4 T cells and MHC-II (OX-6) cells; however, BDC-2.5.*Ncf1*^{m1J} splenocytes displayed a severe reduction in DMPO adducts within CD4 and MHC-II compartments compared with BDC-2.5 (Fig. 2*A*). In the absence of DMPO addition to antigen-stimulated BDC-2.5 and BDC-2.5.*Ncf1*^{m1J} splenocytes, immunofluorescence detection of free radical adducts was absent (Supplementary Fig. 3). The diminution in DMPO-adduct synthesis by BDC-2.5.*Ncf1*^{m1J} CD4- and MHC-II–expressing cells was significant upon quantification, further corroborating reduced respiratory burst activity by

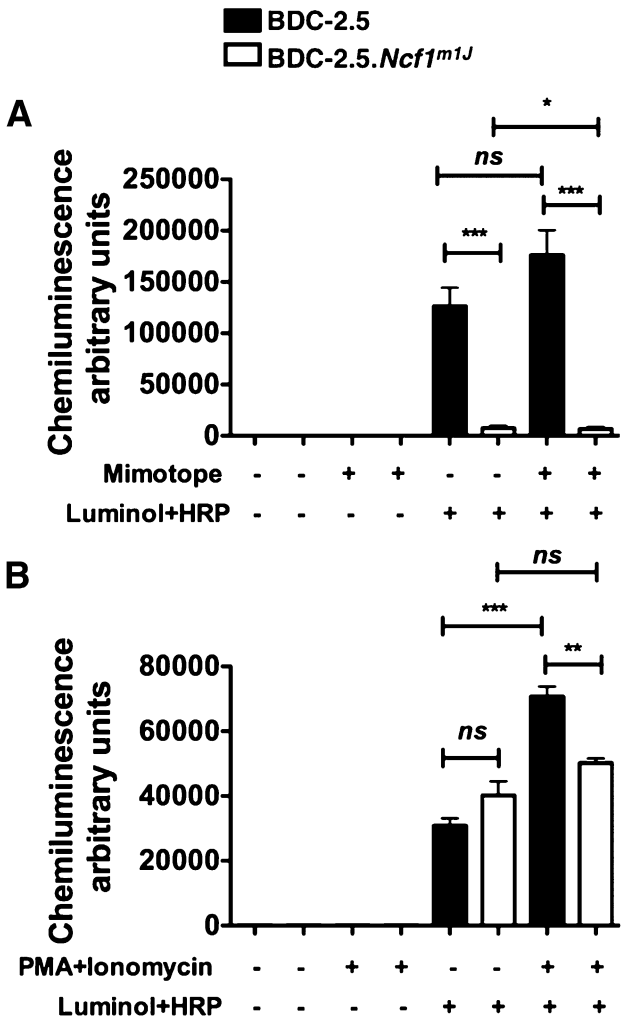

Figure 1—BDC-2.5.*Ncf1*^{m1J} CD4 T cells and splenocytes displayed blunted respiratory burst capacity. Luminol-oxidized chemiluminescence of 5 × 10^5 BDC-2.5 and BDC-2.5.*Ncf1*^{m1J} splenocytes stimulated with 1 μmol/L BDC-2.5 mimotope was analyzed after addition of luminol and HRP (*A*). Luminol-oxidized chemiluminescence of 5 × 10^5 BDC-2.5 and BDC-2.5.*Ncf1*^{m1J} CD4 T cells stimulated with 100 ng/mL PMA and 1 μg/mL ionomycin was assessed post–luminol and HRP addition (*B*). Data shown represent average of 3 experiments performed in triplicate. ns, not significant. ***$P < 0.0001$; **$P < 0.01$; *$P < 0.05$.

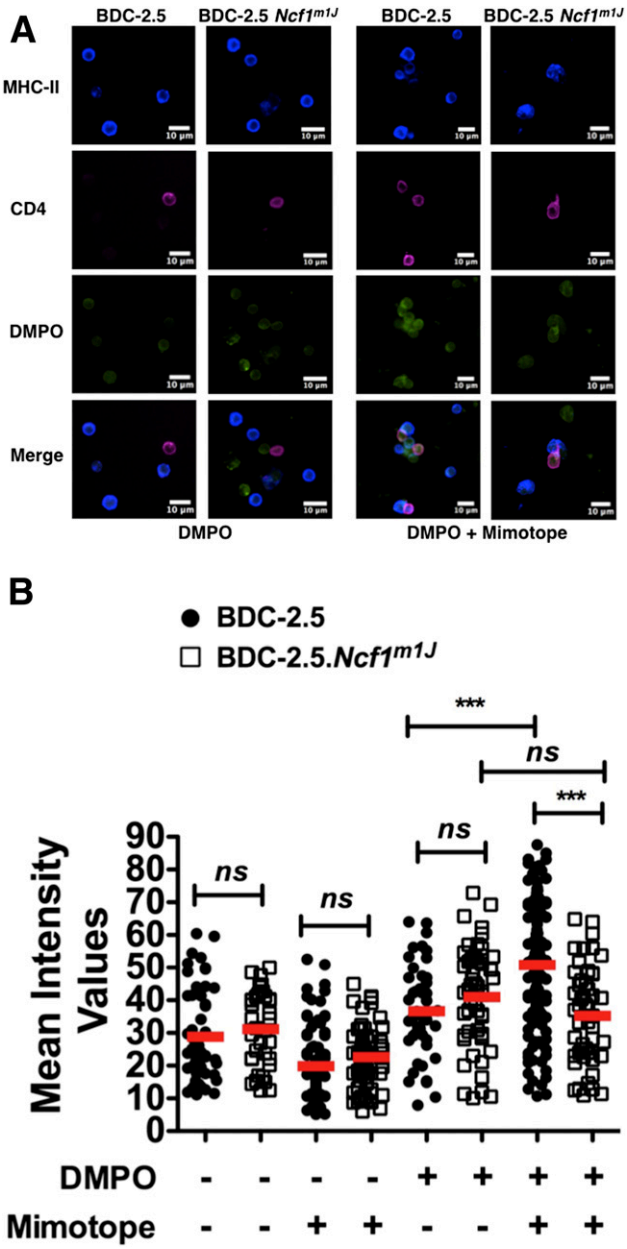

Figure 2—BDC-2.5.*Ncf1*^{m1J} CD4 T cells exhibited reduced macromolecule-centered free radical formation upon antigen stimulation. Immunofluorescence identification of CD4 T cells (Alexa Fluor 647), MHC-II (OX-6; phycoerythrin), and DMPO adducts (Alexa Fluor 488) by BDC-2.5 and BDC-2.5.*Ncf1*^{m1J} splenocytes stimulated with 1 μmol/L BDC-2.5 mimotope with 1 mmol/L DMPO for 12 h (*A*). The fluorescence intensity of DMPO adducts by immune cells was quantitated with ImageJ software (*B*). Data shown represent average of 3 experiments performed in triplicate with the following total number of counted cells per group: BDC-2.5 + DMPO, $n = 46$; BDC-2.5.*Ncf1*^{m1J} + DMPO, $n = 52$; BDC-2.5 + mimotope + DMPO, $n = 118$; BDC-2.5.*Ncf1*^{m1J} + mimotope + DMPO, $n = 51$; BDC-2.5, $n = 52$; BDC-2.5.*Ncf1*^{m1J}, $n = 35$; BDC-2.5 + mimotope, $n = 82$; BDC-2.5.*Ncf1*^{m1J} + mimotope, $n = 66$). Images were magnified at ×40 and digitally enlarged. ns, not significant. ***$P < 0.0001$.

NOX-deficient BDC-2.5 CD4 T cells upon stimulation with their cognate antigen (Fig. 2*B*).

BDC-2.5.*Ncf1*^{m1J} Splenocytes and CD4 T Cells Exhibited Enhanced Synthesis of NO_2^- and Proinflammatory Cytokines and Chemokines

For investigation of the role of NOX-derived superoxide in diabetogenic CD4 T cells, BDC-2.5 and BDC-2.5.*Ncf1*^{m1J} splenocytes were stimulated with dispersed NOD.*Rag* islet cells and the BDC-2.5 mimotope. Contrary to results from our laboratory and others implicating ROS as a proinflammatory-derived third signal essential for effective adaptive immunity (8–10,14), BDC-2.5.*Ncf1*^{m1J} splenocytes displayed significant elevations in nitrite (NO_2^-) (2.7-fold), IFN-γ (4.3- and 2.0-fold), TNF-α (4- and 1.7-fold), IL-1β

(1.5- and 2.5-fold), IL-17A (3.0- and 2.0-fold), and IL-2 (2- and 1.5-fold) upon islet and mimotope stimulation, respectively, compared with BDC-2.5 (Fig. 3*A–F*). Besides an influx in pathogenic proinflammatory cytokines that contribute to β-cell demise and T1D autoreactivity in T1D, BDC-2.5.*Ncf1*^{m1J} splenocytes displayed enhanced synthesis of proinflammatory chemokines implicated in T1D pathogenesis, including CCL5 (chemokine [C-C] motif ligand 5) (3- and 2.0-fold) and CXCL10 (chemokine [C-X-C motif] ligand 10) (332- and 2.0-fold) upon incubation with dispersed islet cells or mimotope, respectively (Fig. 3*G–H*) (29–31). In addition to splenocytes, purified BDC-2.5.*Ncf1*^{m1J} CD4 T cells exhibited significant elevations in nitrite (3.8-fold), IFN-γ (2.8-fold), TNF-α (twofold), IL-1β (4.4-fold), IL-17A (4.5-fold), IL-2 (1.5-fold), CCL5 (2.9-fold), and CXCL10 (twofold) (Supplementary Fig. 4*A–H*). Thus, despite possessing deficiencies in NOX-derived superoxide, BDC-2.5.*Ncf1*^{m1J} splenocytes and CD4 T cells displayed

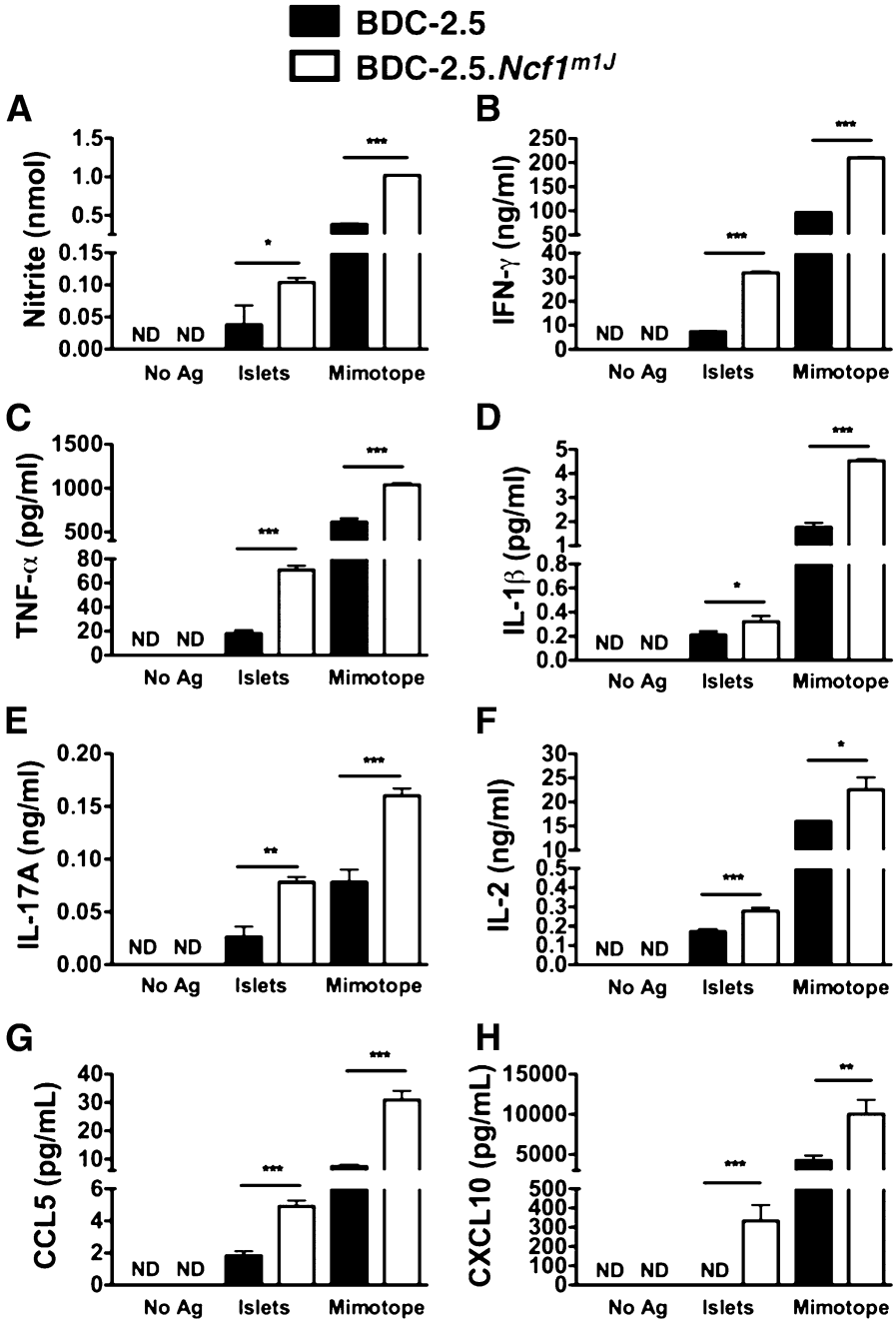

Figure 3— BDC-2.5.*Ncf1*^{m1J} splenocytes displayed an upregulated proinflammatory effector response. Supernatants from BDC-2.5 and BDC-2.5.*Ncf1*^{m1J} splenocytes stimulated with dispersed NOD.*Rag* islets or 1 μmol/L BDC-2.5 mimotope for 48, 72, and 96 h were assayed for synthesis of nitrite (96 h) (*A*), IFN-γ (72 h) (*B*) , TNF-α (72 h) (*C*), IL-1β (96 h) (*D*), IL-17A (48 h) (*E*), IL-2 (72 h) (*F*), CCL5 (72 h) (*G*), and CXCL10 (72 h) (*H*). Data shown represent average of 3 experiments performed in triplicate. Ag, antigen; ND, not detected. ***$P < 0.0001$; **$P < 0.01$; *$P < 0.05$.

elevated levels of proinflammatory mediators implicated in T1D pathogenesis.

BDC-2.5.*Ncf1*^{m1J} CD4 T Cells Exhibited Elevated Activation Markers

For further demonstration that BDC-2.5.*Ncf1*^{m1J} CD4 T cells display an exacerbated effector response in contrast to BDC-2.5, expression of the T-cell activation markers CD69, CD25, and CD44 was assessed by flow cytometry after antigenic stimulation (Fig. 4). Superoxide-deficient BDC-2.5 CD4 T cells exhibited an increase in surface expression of CD69 (early activation marker) (Fig. 4*A*), a 1.6-fold elevation in the IL-2 receptor α-chain (CD25) (Fig. 4*B*), and a 1.3-fold elevation in percentage of CD44 (Fig. 4*C*), a cell-surface glycoprotein that marks effector memory CD4 T cells (32). Pooled data from activated BDC-2.5.*Ncf1*^{m1J} CD4 T cells further demonstrated a significant ($P < 0.05$) increase in CD69 (A), CD25 (B), and CD44 (C) T-cell activation markers in contrast to BDC-2.5 (Supplementary Fig. 7). In agreement with increased proinflammatory cytokine and chemokine synthesis by stimulated BDC-2.5.*Ncf1*^{m1J} T cells (Fig. 3 and Supplementary Fig. 4), the inherent absence of NOX-derived superoxide synthesis elicited an elevated T-cell activation phenotype.

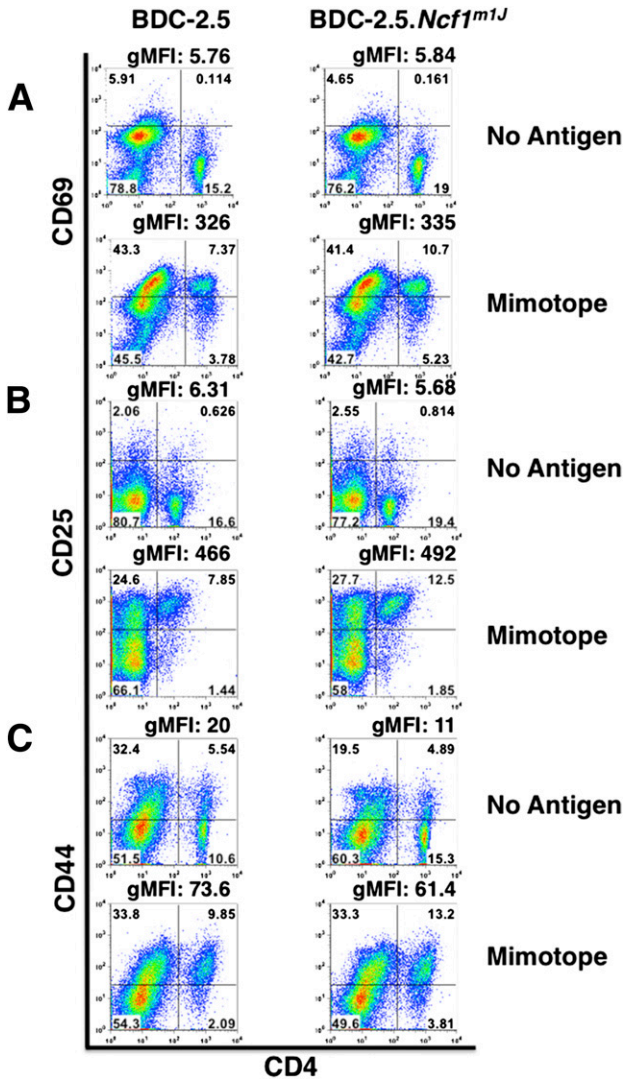

Figure 4—BDC-2.5.*Ncf1*^{m1J} CD4 T cells exhibited increased expression of T-cell activation markers. Flow cytometric analysis of CD69 (*A*), CD25 (*B*), and CD44 (*C*) by live BDC-2.5 and BDC-2.5.*Ncf1*^{m1J} CD4 T cells upon mimotope stimulation for 24 h. Lymphocytes were gated using forward-scatter and side-scatter profiles, while live cells were gated via side-scatter profiles using a fixable live/dead stain (Invitrogen). FACS plots represent data from 3 independent experiments.

BDC-2.5.*Ncf1*^{m1J} Mice Developed Spontaneous T1D and Enhanced Diabetogenicity Upon Adoptive Transfer With Purified BDC-2.5.Ncf1^{m1J} CD4 T Cells

For further demonstration that loss of NOX-derived superoxide can augment CD4 T-cell effector responses, spontaneous T1D incidence was compared between BDC-2.5 and BDC-2.5.*Ncf1*^{m1J} mice. While BDC-2.5 mice do not spontaneously develop autoimmune diabetes, 20% of BDC-2.5.*Ncf1*^{m1J} female mice were hyperglycemic at 30 weeks of age (Fig. 5*A*). For examination of the influence of NOX-derived superoxide on CD4 T-cell diabetogenicity, adoptive transfers of purified, preactivated BDC-2.5 and BDC-2.5.*Ncf1*^{m1J} CD4 T cells into NOD.*Rag* recipients were performed (Fig. 5*B*). Because of the enhanced synthesis of proinflammatory cytokines and chemokines by BDC-2.5.*Ncf1*^{m1J} splenocytes (Fig. 3) and CD4 T cells (Supplementary Fig. 4), we hypothesized that adoptive transfer of superoxide-deficient CD4 T cells would elicit enhanced diabetogenicity compared with BDC-2.5 (21,33). Indeed, transfer of BDC-2.5.*Ncf1*^{m1J} CD4 T cells was more diabetogenic. Only 26% of BDC-2.5.*Ncf1*^{m1J}-transferred NOD.*Rag* ($n = 45$) recipients remained diabetes free at 11 days posttransfer. In contrast, 56% of BDC-2.5–transferred NOD.*Rag* mice ($n = 24$) (Fig. 5*B*) did not develop T1D. However, at 31 days posttransfer, no significant difference in diabetogenicity was observed among the groups of NOD.*Rag* mice receiving BDC-2.5 or BDC-2.5.*Ncf1*^{m1J} CD4 T cells (Fig. 5*B*).

For determination of whether the observed enhanced diabetogenicity could be due to an intrinsic defect in Treg suppressive function, splenic BDC-2.5 and BDC-2.5.*Ncf1*^{m1J} Treg cells were purified and used in an in vivo suppression assay with effector CD4 T cells isolated from BDC-2.5 mice (Fig. 5*C*). Coadoptive transfers into NOD.*Rag* recipients demonstrated that, as expected (34), BDC-2.5 Treg cells were functional and capable of significantly delaying T1D. The majority of the NOD.*Rag* mice transferred with BDC-2.5 Treg cells remained diabetes free (7 of 10 at 30 days posttransfer). However, BDC-2.5.*Ncf1*^{m1J} Treg cells were compromised in their ability to delay T1D. This in vivo suppression assay resulted in only 33% of the NOD.*Rag* recipients remaining diabetes free ($n = 9$) at 30 days postcotransfer (Fig. 5*C*) even though the percentage of Foxp3$^+$ CD4$^+$ CD25$^+$ GITR$^+$ T cells was similar from purified BDC-2.5 and BDC-2.5.*Ncf1*^{m1J} splenic Treg cells (Supplementary Fig. 8).

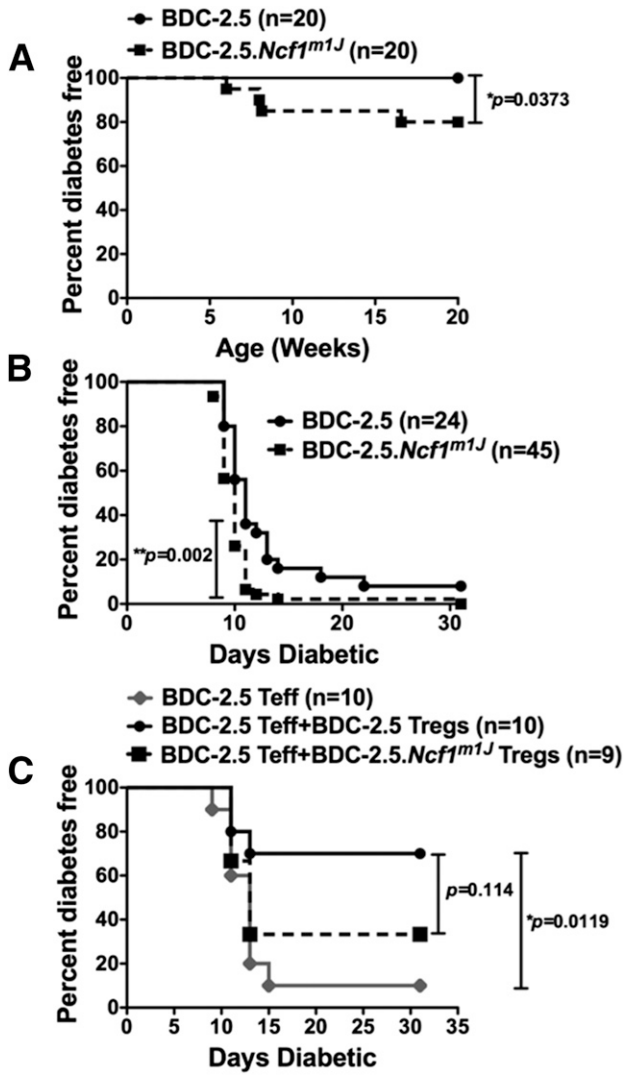

Figure 5—BDC-2.5.*Ncf1*^{m1J} mice developed spontaneous T1D, and adoptive transfer of BDC-2.5.*Ncf1*^{m1J} CD4 T cells was more diabetogenic due to less suppressive Tregs. Kaplan-Meier survival curve of BDC-2.5 (n = 20) and BDC-2.5.*Ncf1*^{m1J} (n = 20) female mice spontaneous incidence (*A*). Kaplan-Meier survival curve of 5×10^6 preactivated and expanded BDC-2.5 or BDC-2.5.*Ncf1*^{m1J} CD4 T cells adoptively transferred into NOD.*Rag* recipients (BDC-2.5, n = 24; BDC-2.5.*Ncf1*^{m1J}, n = 45) (*B*). Kaplan-Meier survival curve of adoptively transferred 10^5 preactivated and expanded BDC-2.5 CD4 T cells alone or with 2×10^4 purified splenic Treg cells from BDC-2.5 or BDC-2.5.*Ncf1*^{m1J} mice into NOD.*Rag* recipients (BDC-2.5, n = 10; BDC-2.5.*Ncf1*^{m1J}, n = 9) (*C*). Mice were considered diabetic with 2 consecutive blood glucose readings ≥300 mg/dL. Data represents compiled incidence from 3 independent experiments. $^{**}P < 0.01$; $^{*}P < 0.05$.

Elevated Proinflammatory Cytokine and Chemokine Synthesis by BDC-2.5.*Ncf1*^{m1J} Was Attenuated by the Addition of an Extrinsic Source of Superoxide

For determination of whether elevated proinflammatory cytokine and chemokine synthesis was directly linked to deficiencies in NOX-derived superoxide, the superoxide-generating enzyme XO was added to BDC-2.5 and BDC-2.5.*Ncf1*^{m1J} splenocytes stimulated with the BDC-2.5 mimotope (Fig. 6*A–E*) or to purified, splenic BDC-2.5 and BDC-2.5.*Ncf1*^{m1J} CD4 T cells stimulated with α-CD3ε and α-CD28 (Fig. 6*F–H*). At 24 h poststimulation with the BDC-2.5 mimotope, BDC-2.5.*Ncf1*^{m1J} splenocytes exhibited a 2.3-fold elevation in IFN-γ synthesis that was blunted by this superoxide donor. XO-mediated superoxide production reduced IFN-γ synthesis levels similar to BDC-2.5 CD4 T cells (Fig. 6*A*). The enhanced levels of TNF-α by stimulated BDC-2.5.*Ncf1*^{m1J} splenocytes were also reduced to wild-type levels with XO addition (Fig. 6*B*). Synthesis of IL-17A was threefold enhanced with mimotope stimulation, but XO addition only slightly attenuated IL-17A production by BDC-2.5.*Ncf1*^{m1J} in comparison with BDC-2.5 (Fig. 6*C*). Further demonstrating the selective decreases in cytokine and chemokine responses by XO addition to stimulated BDC-2.5.*Ncf1*^{m1J} splenocytes, synthesis of the T-cell growth factor IL-2 remained unchanged with this superoxide donor (Fig. 6*D*). CCL5 synthesis was regulated by redox status, as XO induced profound reductions in CCL5 by both stimulated BDC-2.5 and BDC-2.5.*Ncf1*^{m1J} splenocytes (Fig. 6*E*). Similar results were obtained with the chemokine CXCL10, with levels below the limit of detection after XO addition (data not shown). In addition to an elevation in effector cytokine and chemokine synthesis, antigen-stimulated BDC-2.5.*Ncf1*^{m1J} splenocytes also displayed a twofold increase in T-cell proliferation as demonstrated by formazan release in an MTT assay, in contrast to BDC-2.5 splenocytes (Supplementary Fig. 9). Interestingly, unlike effector cytokine synthesis, addition of XO did not decrease T-cell proliferation of mimotope-stimulated BDC-2.5 and BDC-2.5.*Ncf1*^{m1J} splenocytes.

For ascertainment of whether exacerbations in IFN-γ by purified BDC-2.5.*Ncf1*^{m1J} CD4 T cells were similarly attributed to defects in NOX-derived superoxide, XO was added to α-CD3ε– and α-CD28–stimulated BDC-2.5 and BDC-2.5.*Ncf1*^{m1J} CD4 T cells (Fig. 6*F–H*). As anticipated, polyclonal stimulation of BDC-2.5.*Ncf1*^{m1J} CD4 T cells elicited a twofold elevation in IFN-γ, but exogenous XO addition dampened IFN-γ production by 1.4-fold to approximately BDC-2.5 levels (Fig. 6*F*). Similar to BDC-2.5.*Ncf1*^{m1J} splenocytes, modulation of redox status did not affect Th17 cytokine responses with BDC-2.5.*Ncf1*^{m1J} CD4 T cells, as production of IL-17A was unchanged with XO addition (Fig. 6*G*). Interestingly, XO addition enhanced IL-2 synthesis with BDC-2.5 and BDC-2.5.*Ncf1*^{m1J} CD4 T cells (Fig. 6*H*). XO did not negatively impact the viability of BDC-2.5 or BDC-2.5.*Ncf1*^{m1J} splenocytes or CD4 T cells, as determined by an MTT assay (data not shown).

BDC-2.5.*Ncf1*^{m1J} Splenocytes Displayed Increased IL-12Rβ2 and P-STAT4 (Y693) Redox-Dependent Expression Upon Mimotope Stimulation Compared with BDC-2.5

For determination of the redox-dependent mechanism of elevated Th1 cytokine responses by BDC-2.5.*Ncf1*^{m1J} (Fig. 3*B*; Supplementary Fig. 4), expression of IL-12Rβ2, a Th1 signal transducer, (Fig. 7 and Supplementary Fig. 10), and

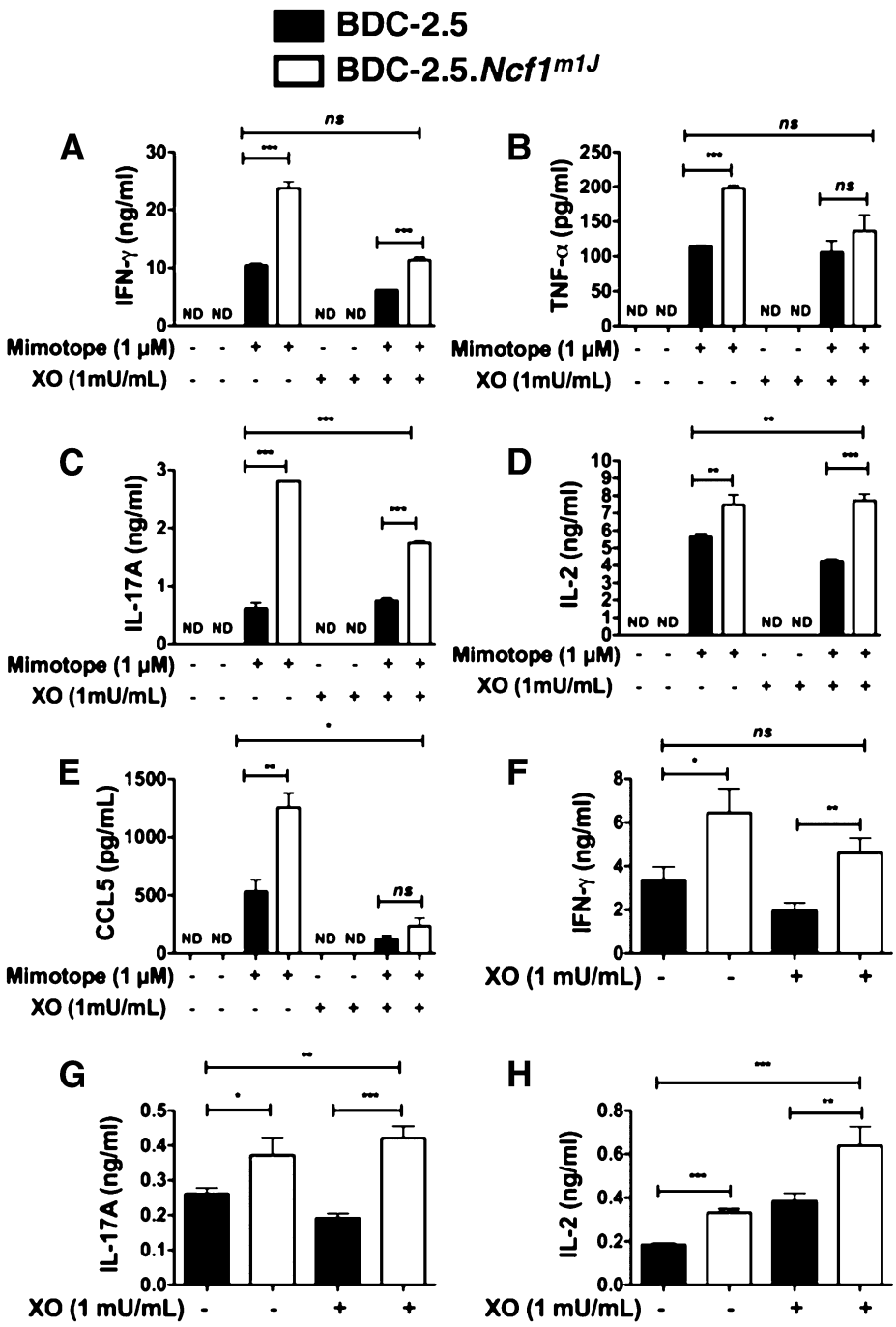

Figure 6—Enhanced proinflammatory cytokine and chemokine synthesis by BDC-2.5.*Ncf1*^{m1J} splenocytes and CD4 T cells was attenuated by xanthine oxidase addition. Supernatants from BDC-2.5 and BDC-2.5.*Ncf1*^{m1J} primary recall assays were assayed for IFN-γ (*A*), TNF-α (*B*), IL-17A (*C*), IL-2 (*D*), and CCL5 (*E*) production upon stimulation with 1 μmol/L mimotope with or without the addition of 1 mU/mL XO for 12 h (IL-17A) and 24 h (IFN-γ, CCL5, and IL-2). Supernatants from BDC-2.5 and BDC-2.5.*Ncf1*^{m1J} CD4 T-cell polyclonal stimulations (0.1 μg/mL α-CD3ε, 1 μg/mL α-CD28) with or without 1 mU/mL XO for 24 h were assayed for IFN-γ (*F*), IL-17A (*G*), and IL-2 (*H*). Data shown represent average of 3 experiments performed in triplicate. ND, not detected; ns, not significant. $^{*}P < 0.05$; $^{**}P < 0.01$; $^{***}P < 0.0001$.

the phosphorylation status of STAT4, a transcription factor essential for Th1 responses (Fig. 8 and Supplementary Fig. 11), were examined via flow cytometry and immunofluorescence, respectively. Mimotope stimulation elicited a 1.5-fold increase in IL-12Rβ2^{+}, CD4^{+} T cells by superoxide-deficient splenocytes and a 1.35-fold elevation in gMFI (geometric mean fluorescence intensity) (Fig. 7). Upon addition of xanthine oxidase, IL-12Rβ2 expression was attenuated by mimotope-stimulated superoxide-deficient CD4 T cells (Fig. 7). Similar to IL-12Rβ2, P-STAT4 (Y693), an essential Th1 transcription factor, was significantly enhanced by BDC-2.5.*Ncf1*^{m1J} (Fig. 8 and Supplementary Fig. 11).

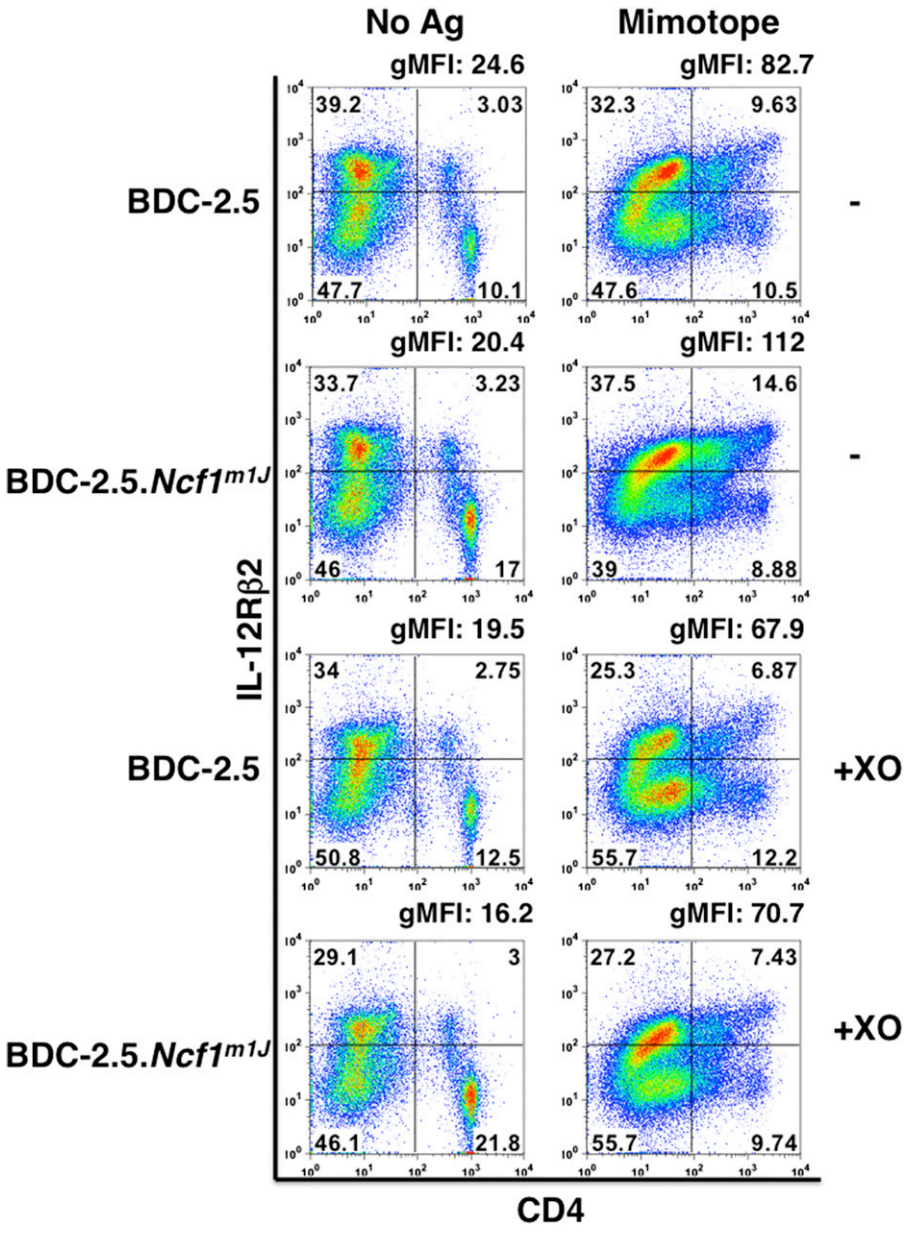

Figure 7—Superoxide donors dampened the expression of IL-12Rβ2. Flow cytometric analysis of IL-12Rβ2 by live BDC-2.5 and BDC-2.5.*Ncf1*^{m1J} CD4 T cells upon mimotope stimulation with or without addition of XO for 72 h. Lymphocytes were gated using forward-scatter and side-scatter profiles, while live cells were gated via side-scatter profiles using a fixable live/dead stain (Invitrogen). IL-12Rβ2 flow cytometry is representative of 2 independent experiments.

With exogenous superoxide addition via XO, P-STAT4 (Y693) was severely diminished to levels similar to NOX-intact BDC-2.5 cells (Fig. 8). Thus, in addition to functioning as a proinflammatory-derived third signal, ROS can attenuate Th1 proinflammatory cytokine responses by lessening IL-12Rβ2 signaling and STAT4 activation.

DISCUSSION

In T1D, ROS directly destroy β-cells and induce proinflammatory cytokines that further propagate β-cell destruction by maturing autoreactive adaptive immune effector responses (35,36). Reports by our laboratory and others have demonstrated that systemic ablation of innate immune-derived ROS results in antigen-specific hyporesponsiveness (8,15). We previously demonstrated that NOD mice defective in NOX-derived superoxide via the spontaneous mutation *Ncf1*^{m1J} were protected against T1D onset due to skewed CD4 T-cell responses (10), reduced CD8 T-cell cytotoxic capacity (18), lessened antiviral proinflammatory responses (17,27), and deviation to an alternatively-activated M2 macrophage phenotype (27). To further define the role of ROS in diabetogenic CD4 T-cell responses, we generated the BDC-2.5.*Ncf1*^{m1J} mouse strain, possessing autoreactive and superoxide-deficient

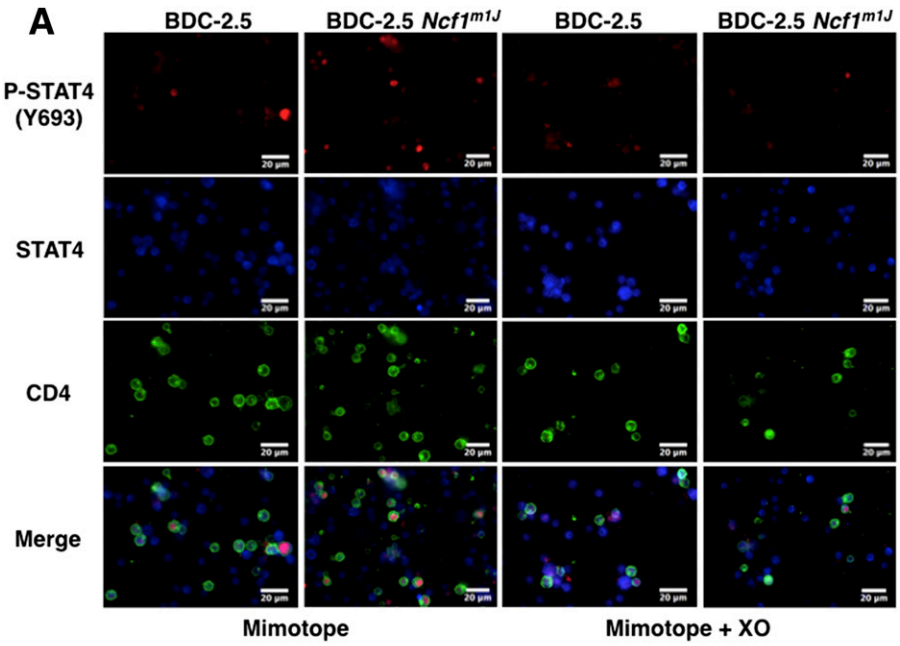

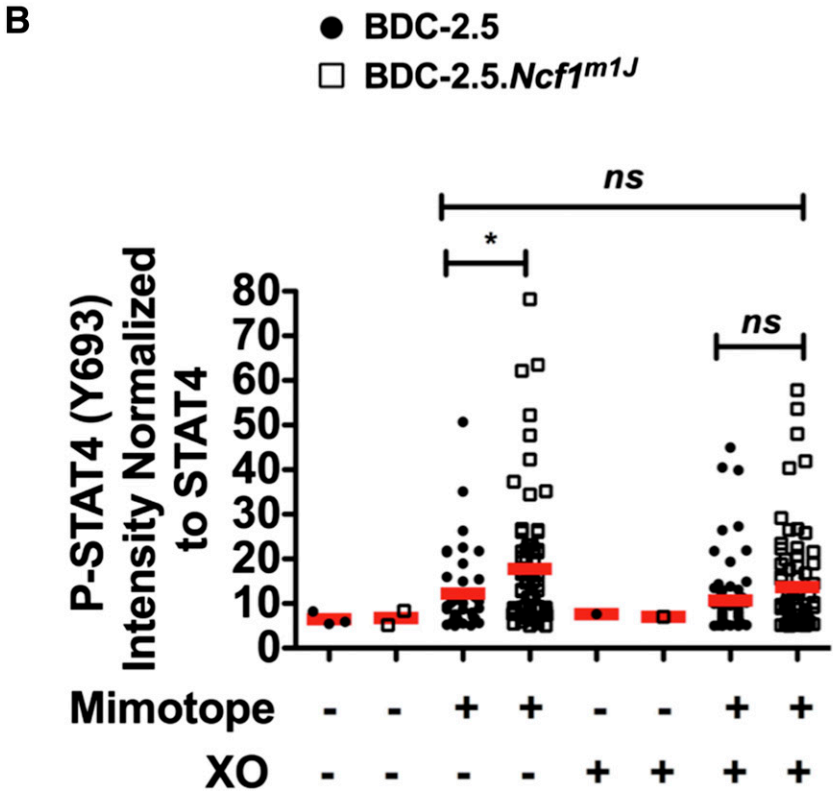

Figure 8—BDC-2.5.*Ncf1*^{m1J} splenocytes exhibited enhanced P-STAT4 (Y693) activation that was curtailed with exogenous superoxide. Immunofluorescence identification of CD4 T cells (Alexa Fluor 647), STAT4 (Cy3), and P-STAT4 (Y693) (Alexa Fluor 488) by BDC-2.5 and BDC-2.5.*Ncf1*^{m1J} splenocytes stimulated with 1 μmol/L BDC-2.5 mimotope with or without 1 mU/mL XO for 24 h (*A*). The fluorescence intensity of P-STAT4 (Y693) by immune cells was quantitated with ImageJ software and normalized to STAT4 (*B*). P-STAT4 (Y693) immunofluorescence is representative of 3 independent experiments with the following total number of counted cells per group: BDC-2.5 no antigen, $n = 278$; BDC-2.5.*Ncf1*^{m1J} no antigen, $n = 570$; BDC-2.5 + mimotope, $n = 652$; BDC-2.5.*Ncf1*^{m1J} + mimotope, $n = 497$; BDC-2.5 + XO, $n = 366$; BDC-2.5.*Ncf1*^{m1J} + XO, $n = 375$; BDC-2.5 + mimotope + XO, $n = 670$; BDC-2.5.*Ncf1*^{m1J} + mimotope + XO, $n = 641$). Images were magnified at 40× and digitally enlarged. ns, not significant. *$P < 0.05$.

CD4 T cells. Because of the unique T1D resistance displayed by NOD.*Ncf1*^{m1J} mice, we hypothesized that BDC-2.5.*Ncf1*^{m1J} CD4 T cells would exhibit decreased effector cytokine synthesis and diabetogenicity. Surprisingly, unlike the reduced Th1 cytokine profile displayed by NOD.*Ncf1*^{m1J}, activated BDC-2.5.*Ncf1*^{m1J} splenocytes and CD4 T cells displayed elevated synthesis of proinflammatory chemokines, Th1 and Th17 cytokines; enhanced diabetogenicity; and reduced Treg suppressive function.

Although initially apparently contradictory, these results are supported by other lines of evidence in additional autoimmune diseases. Deficiencies in NOX-derived superoxide have been shown to enhance autoimmunity in animal models of autoimmune arthritis (37,38), multiple sclerosis (10,37), Crohn disease (39), systemic lupus erythematosus (40), and psoriasis (41). With the aid of the NOD.BDC-2.5.*Ncf1*^{m1J} high-affinity TCR transgenic murine model, we can now include NOX-derived superoxide as a novel immunoregulatory molecule of diabetogenic CD4 T cell responses and pancreatic β-cell destruction in T1D. In addition to enhanced proinflammatory cytokine and chemokine synthesis, we report that BDC-2.5.*Ncf1*^{m1J} CD4 T cells were more diabetogenic during spontaneous and adoptive transfer of T1D, due to trending reductions in Treg-mediated immunosuppression. Our data corroborate a previous report of defective immunoregulation by Tregs possessing the *Ncf1*^{m1J} mutation (42). Additionally, rodents bearing a spontaneous mutation in the *Ncf1*^{m1J} gene were more susceptible to autoimmune arthritis (37), and administration of the ROS donor phytol curbed arthritogenic T-cell responses (43). Similarly, we demonstrated that T1D-resistant NOD.*Ncf1*^{m1J} mice exhibited enhanced sensitivity to myelin oligodendrocyte glycoprotein ($MOG_{35–55}$)-induced experimental autoimmune encephalomyelitis (10). Analogous to murine models, chronic granulomatous disease patients, harboring mutations in the phagocyte NOX complex, possessed an elevated type I interferon gene signature, increased synthesis of proinflammatory cytokines (i.e., IL-17A) and chemokines (40), macrophages that were profoundly less efficient in inducing Tregs compared with healthy controls (44), and an elevated risk of developing autoimmunity (45–47). These results provide evidence that NOX-derived superoxide can negatively regulate effector T-cell and B-cell responses in various autoimmune diseases.

Recent studies by our laboratory demonstrated that NOD.*Ncf1*^{m1J} CD4 T cells were equally pathogenic as NOD CD4 T cells, as cotransfers of purified NOD.*Ncf1*^{m1J} CD4 T cells with NOD CD8 T cells resulted in rapid T1D-onset kinetics (18). These results provide evidence that NOX-derived superoxide is involved in peripheral tolerance and elicits a redox-dependent signaling cue to halt diabetogenic CD4 T cells. ROS synthesis negatively impacted IL-12Rβ2 signaling and STAT4 activation, providing mechanistic insight to the process whereby ROS can blunt CD4 T-cell activation. Our results provide evidence that moderate increases in oxidative stress may be beneficial as an essential checkpoint to curtail T cell–mediated diseases dominated by Th1 cytokine responses, such as T1D.

Here, we demonstrate that NOX-deficient CD4 T cells bearing a high-affinity autoreactive T-cell receptor exhibited elevated IFN-γ production. This is in conflict with our previous observation that IFN-γ was blunted in the absence of NOX-derived superoxide by polyclonal NOD.*Ncf1*^{m1J} CD4 T cells (10). This difference in Th1 responses could be attributed to inherent disparities in T-cell phenotype. NOD CD4 T-cell responses are polyclonal, characterized by distinct avidities to different autoantigens, while BDC-2.5 CD4 T cells are inherently skewed to a Th1-like phenotype and recognize a single autoantigen, chromogranin A (21,22). NOD mice spontaneously develop T1D, whereas BDC-2.5 mice exhibit a low incidence due to immunosuppressive Treg cells (34). Enhanced Th1 cytokine responses have not only been observed within BDC-2.5.*Ncf1*^{m1J} CD4 T cells; our preliminary data also demonstrate that BDC-6.9, another diabetogenic CD4 T cell clone that recognizes islet amyloid polypeptide (IAPP) (48), exhibits an enhanced Th1 and Th17 cytokine response in the absence of NOX-derived superoxide (L.E. Padgett, N.N. Morgan, and H.M. Tse, unpublished data). These monoclonal TCR transgenic murine models of T1D have enabled us to uncover the importance of ROS in T-cell effector inhibition, and thus, similar to rheumatoid arthritis (RA) (37,38), multiple sclerosis (10,37), Crohn disease, psoriasis (41), and systemic lupus erythematosus (40), increasing the production of free radicals by CD4 T cells may be efficacious in T1D.

The disparate in vitro Th1 responses by NOD.*Ncf1*^{m1J} and BDC-2.5.*Ncf1*^{m1J} could additionally be attributed to differences in inherent levels of ROS and sensitivity of immune cells to redox-dependent signaling. Illustrative of the inherent dissimilarity in redox status, BDC-2.5.*Ncf1*^{m1J} CD4 T cells displayed elevated nitrite, but no difference was observed in NOD and NOD.*Ncf1*^{m1J} CD4 T cells (10). A profound mechanism by which ROS influence T-cell effector responses at the immunological synapse is by reversibly oxidizing thiol residues located within TCR adaptor molecules. TCR adaptor molecules are regulated by redox status and, more importantly, T-bet, the master transcription factor involved in Th1 cytokine responses, is also influenced by ROS synthesis (10). Future studies will dissect differences in redox-dependent signaling by exploring TCR adaptor molecule oxidation status within NOD.*Ncf1*^{m1J} and BDC-2.5.*Ncf1*^{m1J} CD4 T cells, as unraveling these may reveal novel targets for T1D protection and prevention.

By using T1D-resistant NOD.*Ncf1*^{m1J} mice lacking the ability to generate NOX-derived superoxide (10), our laboratory has defined an influential role for free radicals on the maturation of autoimmune responses in T1D. We have mechanistically determined that the induction of innate immune signaling pathways and differentiation of islet-resident and islet-infiltrating proinflammatory

M1 macrophages are dependent on NOX-derived superoxide during spontaneous T1D (10,17,18,27). The absence of superoxide can skew macrophage responses toward an alternatively activated M2 phenotype and elicit β-cell protection. However, the role of NOX-derived superoxide on T cells is more complex. Free radicals may have distinct effects on T-cell subsets, in addition to expansion, contraction, and memory formation. CD8 T cells from NOD.*Ncf1*^{m1J} mice are impaired and unable to transfer T1D (10,18). These observations would suggest that CD8 T cells are highly dependent on NOX-derived superoxide as a signaling mediator for cytotoxic lymphocyte maturation. CD4 T cells from NOD.*Ncf1*^{m1J} mice also require superoxide as a third signal to efficiently generate Th1 cytokine-producing cells (10), but within a subset of high-affinity autoreactive T cells (BDC-2.5, BDC-6.9), NOX-derived superoxide may also be necessary as a checkpoint to quell T-cell effector responses, facilitate T-cell contraction, and/or restore peripheral tolerance in T1D. Our studies further define the synergism of redox biology in autoimmune dysregulation in T1D and may lead to the development of novel immunotherapies to delay disease progression.

Acknowledgments. The authors are grateful to Stew New from the Department of Microbiology at University of Alabama at Birmingham (UAB) for technical assistance with ImageJ and immunofluorescence assays. The authors thank Ashley Burg (Department of Microbiology) and Shaonli Das (Department of Microbiology), Chad Hunter (Department of Medicine), and Sasanka Ramanadham (Department of Cell, Developmental and Integrative Biology) from UAB for critical reading of the manuscript.

Funding. This work was supported by a National Institutes of Health (NIH)/National Institute of Diabetes and Digestive and Kidney Diseases (NIDDK) R01 award (DK-099550), an American Diabetes Association Career Development Award (7-12-CD-11), a P30 Pilot Feasibility award from the UAB Comprehensive Diabetes Center/Diabetes Research Training Center, an NIH National Institute of Allergy and Infectious Diseases (5T32AI007051-35) Immunologic Diseases and Basic Immunology T32 training grant (to L.E.P.), and a Travel for Techniques Program Award from the American Association for Immunologists, Inc. (to H.M.T.). Further support was provided by an NIH/NIDDK R01 award (DK-074656) and a grant from the JDRF (to C.E.M.). This research was partially supported by the Intramural Research Program of the National Institute of Environmental Health Sciences/NIH. The following core facilities of UAB were used to generate data for the manuscript: Animal Resources Program (G20RR025858, Sam Cartner); the Comprehensive Arthritis, Musculoskeletal, and Autoimmunity Center: Analytic and Preparative Cytometry Facility (P30 AR48311, John D. Mountz); and the Comprehensive Arthritis, Musculoskeletal, and Autoimmunity Center: Epitope Recognition Immunoreagent Core (P30 AR48311, Mary Ann Accavitti-Loper).

Duality of Interest. No potential conflicts of interest relevant to this article were reported.

Author Contributions. L.E.P. researched data, wrote the manuscript, and reviewed and edited the manuscript. B.A. researched data and reviewed and edited the manuscript. C.L. researched data. D.G. researched data and reviewed and edited the manuscript. R.P.M. and J.D.P. reviewed and edited the manuscript. C.E.M. reviewed and edited the manuscript and contributed to discussion. H.M.T. researched data, wrote the manuscript, and reviewed and edited the manuscript. H.M.T. is the guarantor of this work and, as such, had full access to all the data in the study and takes responsibility for the integrity of the data and the accuracy of the data analysis.

References

1. Patterson CC, Gyürüs E, Rosenbauer J, et al. Trends in childhood type 1 diabetes incidence in Europe during 1989-2008: evidence of non-uniformity over time in rates of increase. Diabetologia 2012;55:2142–2147
2. Patterson CC, Dahlquist GG, Gyürüs E, Green A, Soltész G; EURODIAB Study Group. Incidence trends for childhood type 1 diabetes in Europe during 1989-2003 and predicted new cases 2005-20: a multicentre prospective registration study. Lancet 2009;373:2027–2033
3. Shizuru JA, Taylor-Edwards C, Banks BA, Gregory AK, Fathman CG. Immunotherapy of the nonobese diabetic mouse: treatment with an antibody to T-helper lymphocytes. Science 1988;240:659–662
4. Thivolet C, Bendelac A, Bedossa P, Bach JF, Carnaud C. CD8+ T cell homing to the pancreas in the nonobese diabetic mouse is CD4+ T cell-dependent. J Immunol 1991;146:85–88
5. Sareila O, Kelkka T, Pizzolla A, Hultqvist M, Holmdahl R. NOX2 complex-derived ROS as immune regulators. Antioxid Redox Signal 2011;15:2197–2208
6. Heyworth PG, Curnutte JT, Nauseef WM, et al. Neutrophil nicotinamide adenine dinucleotide phosphate oxidase assembly. Translocation of p47-phox and p67-phox requires interaction between p47-phox and cytochrome b558. J Clin Invest 1991;87:352–356
7. Lam GY, Huang J, Brumell JH. The many roles of NOX2 NADPH oxidase-derived ROS in immunity. Semin Immunopathol 2010;32:415–430
8. Tse HM, Milton MJ, Piganelli JD. Mechanistic analysis of the immunomodulatory effects of a catalytic antioxidant on antigen-presenting cells: implication for their use in targeting oxidation-reduction reactions in innate immunity. Free Radic Biol Med 2004;36:233–247
9. Tse HM, Milton MJ, Schreiner S, Profozich JL, Trucco M, Piganelli JD. Disruption of innate-mediated proinflammatory cytokine and reactive oxygen species third signal leads to antigen-specific hyporesponsiveness. J Immunol 2007;178:908–917
10. Tse HM, Thayer TC, Steele C, et al. NADPH oxidase deficiency regulates Th lineage commitment and modulates autoimmunity. J Immunol 2010;185:5247–5258
11. Curtsinger JM, Lins DC, Johnson CM, Mescher MF. Signal 3 tolerant CD8 T cells degranulate in response to antigen but lack granzyme B to mediate cytolysis. J Immunol 2005;175:4392–4399
12. Curtsinger JM, Lins DC, Mescher MF. Signal 3 determines tolerance versus full activation of naive CD8 T cells: dissociating proliferation and development of effector function. J Exp Med 2003;197:1141–1151
13. Curtsinger JM, Valenzuela JO, Agarwal P, Lins D, Mescher MF. Type I IFNs provide a third signal to CD8 T cells to stimulate clonal expansion and differentiation. J Immunol 2005;174:4465–4469
14. Curtsinger JM, Mescher MF. Inflammatory cytokines as a third signal for T cell activation. Curr Opin Immunol 2010;22:333–340
15. Piganelli JD, Flores SC, Cruz C, et al. A metalloporphyrin-based superoxide dismutase mimic inhibits adoptive transfer of autoimmune diabetes by a diabetogenic T-cell clone. Diabetes 2002;51:347–355
16. Huang CK, Zhan L, Hannigan MO, Ai Y, Leto TL. P47(phox)-deficient NADPH oxidase defect in neutrophils of diabetic mouse strains, C57BL/6J-m db/db and db/+. J Leukoc Biol 2000;67:210–215
17. Seleme MC, Lei W, Burg AR, et al. Dysregulated TLR3-dependent signaling and innate immune activation in superoxide-deficient macrophages from nonobese diabetic mice. Free Radic Biol Med 2012;52:2047–2056
18. Thayer TC, Delano M, Liu C, et al. Superoxide production by macrophages and T cells is critical for the induction of autoreactivity and type 1 diabetes. Diabetes 2011;60:2144–2151
19. Padgett LE, Burg AR, Lei W, Tse HM. Loss of NADPH oxidase-derived superoxide skews macrophage phenotypes to delay type 1 diabetes. Diabetes 2015;64:937–946
20. Haskins K, Portas M, Bergman B, Lafferty K, Bradley B. Pancreatic islet-specific T-cell clones from nonobese diabetic mice. Proc Natl Acad Sci U S A 1989;86:8000–8004

21. Katz JD, Wang B, Haskins K, Benoist C, Mathis D. Following a diabetogenic T cell from genesis through pathogenesis. Cell 1993;74:1089–1100
22. Stadinski BD, Delong T, Reisdorph N, et al. Chromogranin A is an autoantigen in type 1 diabetes. Nat Immunol 2010;11:225–231
23. Calderon B, Suri A, Unanue ER. In CD4+ T-cell-induced diabetes, macrophages are the final effector cells that mediate islet beta-cell killing: studies from an acute model. Am J Pathol 2006;169:2137–2147
24. Cantor J, Haskins K. Recruitment and activation of macrophages by pathogenic CD4 T cells in type 1 diabetes: evidence for involvement of CCR8 and CCL1. J Immunol 2007;179:5760–5767
25. Ramirez DC, Mason RP. Immuno-spin trapping: detection of protein-centered radicals. Curr Protoc Toxicol 2005;Chapter 17:Unit 17.7
26. Mason RP. Using anti-5,5-dimethyl-1-pyrroline N-oxide (anti-DMPO) to detect protein radicals in time and space with immuno-spin trapping. Free Radic Biol Med 2004;36:1214–1223
27. Padgett LE, Burg AR, Lei W, Tse HM: Loss of NADPH oxidase-derived superoxide skews macrophage phenotypes to delay type 1 diabetes. Diabetes 2015;64:937–946
28. Jackson SH, Devadas S, Kwon J, Pinto LA, Williams MS. T cells express a phagocyte-type NADPH oxidase that is activated after T cell receptor stimulation. Nat Immunol 2004;5:818–827
29. Jamali Z, Nazari M, Khoramdelazad H, et al. Expression of CC chemokines CCL2, CCL5, and CCL11 is associated with duration of disease and complications in type-1 diabetes: a study on Iranian diabetic patients. Clin Lab 2013;59:993–1001
30. Roep BO, Kleijwegt FS, van Halteren AG, et al. Islet inflammation and CXCL10 in recent-onset type 1 diabetes. Clin Exp Immunol 2010;159:338–343
31. Uno S, Imagawa A, Okita K, et al. Macrophages and dendritic cells infiltrating islets with or without beta cells produce tumour necrosis factor-alpha in patients with recent-onset type 1 diabetes. Diabetologia 2007;50:596–601
32. DeGrendele HC, Kosfiszer M, Estess P, Siegelman MH. CD44 activation and associated primary adhesion is inducible via T cell receptor stimulation. J Immunol 1997;159:2549–2553
33. Haskins K, McDuffie M. Acceleration of diabetes in young NOD mice with a CD4+ islet-specific T cell clone. Science 1990;249:1433–1436
34. Feuerer M, Shen Y, Littman DR, Benoist C, Mathis D. How punctual ablation of regulatory T cells unleashes an autoimmune lesion within the pancreatic islets. Immunity 2009;31:654–664
35. Thomas HE, McKenzie MD, Angstetra E, Campbell PD, Kay TW. Beta cell apoptosis in diabetes. Apoptosis 2009;14:1389–1404
36. Meares GP, Fontanilla D, Broniowska KA, Andreone T, Lancaster JR Jr, Corbett JA. Differential responses of pancreatic β-cells to ROS and RNS. Am J Physiol Endocrinol Metab 2013;304:E614–E622
37. Hultqvist M, Olofsson P, Holmberg J, Bäckström BT, Tordsson J, Holmdahl R. Enhanced autoimmunity, arthritis, and encephalomyelitis in mice with a reduced oxidative burst due to a mutation in the Ncf1 gene. Proc Natl Acad Sci U S A 2004;101:12646–12651
38. Olofsson P, Holmberg J, Tordsson J, Lu S, Akerström B, Holmdahl R. Positional identification of Ncf1 as a gene that regulates arthritis severity in rats. Nat Genet 2003;33:25–32
39. Conway KL, Goel G, Sokol H, et al. p40phox expression regulates neutrophil recruitment and function during the resolution phase of intestinal inflammation. J Immunol 2012;189:3631–3640
40. Kelkka T, Kienhöfer D, Hoffmann M, et al. Reactive oxygen species deficiency induces autoimmunity with type 1 interferon signature. Antioxid Redox Signal 2014;21:2231–2245
41. Kim HR, Lee A, Choi EJ, et al. Reactive oxygen species prevent imiquimod-induced psoriatic dermatitis through enhancing regulatory T cell function. PLoS One 2014;9:e91146
42. Efimova O, Szankasi P, Kelley TW. Ncf1 (p47phox) is essential for direct regulatory T cell mediated suppression of CD4+ effector T cells. PLoS One 2011;6:e16013
43. Hultqvist M, Olofsson P, Gelderman KA, Holmberg J, Holmdahl R. A new arthritis therapy with oxidative burst inducers. PLoS Med 2006;3:e348
44. Kraaij MD, Savage ND, van der Kooij SW, et al. Induction of regulatory T cells by macrophages is dependent on production of reactive oxygen species. Proc Natl Acad Sci U S A 2010;107:17686–17691
45. Badolato R, Notarangelo LD, Plebani A, Roos D. Development of systemic lupus erythematosus in a young child affected with chronic granulomatous disease following withdrawal of treatment with interferon-gamma. Rheumatology (Oxford) 2003;42:804–805
46. De Ravin SS, Naumann N, Cowen EW, et al. Chronic granulomatous disease as a risk factor for autoimmune disease. J Allergy Clin Immunol 2008;122:1097–1103
47. Lee BW, Yap HK. Polyarthritis resembling juvenile rheumatoid arthritis in a girl with chronic granulomatous disease. Arthritis Rheum 1994;37:773–776
48. Delong T, Baker RL, He J, Haskins K. Novel autoantigens for diabetogenic CD4 T cells in autoimmune diabetes. Immunol Res 2013;55:167–172